Journal of
Polymer & Composites

ISSN: 2321-2810 (Online)
ISSN: 2321-8525 (Print)
Volume 13, Special Issue 5, 2025
DOI (Journal): 10.37591/JoPC

https://journals.stmjournals.com/jopc

Research JoPC

Process Parameters Optimization of Fiber Laser Cladded SS316 Surface Using RSM Analysis

Vikas Kumar [1,*], Ravi Shankar Rai [2], Rajeev Kumar [3]

Abstract

This paper presents the laser cladding experiments on the surface of SS316 to study the variations in process parameters, such as scanning speed (100-250 mm/min), laser power (50-250 W), and % volume of B_4C (5- 25%) + SS316 powder on the mechanical, metallurgical and tribological performance of the modified surface. A central composite design (CCD) was used to develop the response surface methodology (RSM) to design the experiments and for analysis of the results. To correlate the input process parameters with the responses, regression equations were formulated. Field Emission Scanning Electron Microscopy (FESEM) observation indicated the uniform distribution of B_4C particles with the absence of fine gaps at the interfaces of SS316 and B_4C particles. X-ray Diffraction analysis revealed that different intermetallic compounds, such FEC, B_4C, B_2O_3, FeNi, Mo_2B, NiMn, FeB, and CrC, were formed during the laser interaction with the surface resulting from chemical reactions. The optimum values of different responses, such as average micro-hardness, coefficient of friction, and clad layer thickness, were found to be 322.05$HV_{0.2}$ (maximum), 0.324(minimum), and 0.376 mm (maximum), respectively, for the predicted input process parameters, namely scanning speed: 172.72 mm/min; laser power: 200 W; and, the composition of B_4C: 20% v/v

Keywords: Fiber laser cladding; SS316; B_4C; microstructure; microhardness; RSM

INTRODUCTION

Surface structures and properties of materials have been an important aspect of industrial evolution. As the industry evolved with the progress of human civilization, mankind developed different materials, which, in turn, became an essential agent of further progress of an era. It is the surface properties or surface features of materials that determine the functionality of a material to a large extent. Particularly, since the advent of the modern industrial era, features, such as, excellent wear resistance, corrosion resistance, hardness, high heat resistance, etc., have become essential qualities for different types of material surfaces. Alloys, i.e., a compound of two or more substances, have traditionally been found to have superior properties compared to pure metals. For instance, alloys are usually very arduous. However, they are also expensive to manufacture. Hence, there has been a consistent effort to rationalize the production process as well as the cost of production of the parts, made of alloys, which have the requisite surface properties. This can be achieved by using the appropriate surface modification technique, which is also known as pre-treatment, treatment and activation of different materials (metals, ceramics, polymers, composite, etc.). During the process, the material is deposited onto the substrate surface under the laser beam by a number of routes including powder blowing, wire feeding, pre-placed powder coating, etc. A major application of laser cladding is in the area of repair and refurbishment of high- value components, such as, tools, turbine blades, gas turbines and internal

***Author for Correspondence**
Vikas Kumar

[1,2]Assistant Professor, Department of Automation and Robotics Engineering, Sandip Institute of Technology and Research Centre, Nashik, Maharashtra, India
[3]Assistant Professor, Department of Mechanical Engineering, Sandip Institute of Technology and Research Centre, Nashik, Maharashtra, India

Received Date: January 16, 2025
Accepted Date: March 18, 2025
Published Date: July 10, 2025

Citation: Vikas Kumar, Ravi Shankar Rai, Rajeev Kumar. Process Parameters Optimization of Fiber Laser Cladded SS316 Surface Using RSM Analysis. Journal of Polymer & Composites. 2025; 13(Special Issue 5): S186–S201p.

combustion engine parts [1-9]. There are many other applications of laser-based direct material deposition, such as, functional coatings, repair depositions, rapid design changes and finally direct generation of 3D parts, made from ferrous/non-ferrous materials medical applications. Lasers are one of the most remarkable inventions of the twentieth century because of their extraordinary characteristics, i.e., high brightness, high directionality, high coherence, high monochromaticity and unique spatial as well as temporal distribution. Process parameters of laser cladding have an important influence on clad surface properties. Liu et al. [10] optimized the process parameters (scanning speed, laser power, powder feeding rate and shielding gas flow rate) of the laser- deposited AlSi10Mg alloy by the Taguchi method to get the optimum density. In the previous literature, the relationship between each process parameter and the quality of the cladding layer was explored separately. To the best of the authors' knowledge, literature related to investigation on the synergic effects of processing parameters and the optimization of process parameters of laser cladding composite material was limited.

MATERIALS AND METHODS

Experimental workstation

The experimental workstation, used in the present study, comprised of fibre laser source, beam delivery system, CNC X-Y-Z stage, gas purging arrangement and to cool down the laser source, chiller unit also attached with the system. Cladding workstation shown in Figure 1.

The cladding experiments were conducted using a continuous mode fiber laser source (model No-SMS00051, (make: SPI Lasers, UK), with power output ranging from 50 - 400 W. It was ytterbium-doped fibre laser. The required power was set by using the graphic user interface, shown in Figure. 2. Specification of the fibre laser source has been provided in Table 1. Figure 3 shows the laser source and beam delivery system.

Substrate and Clad Materials

In the current study SS316 taken as substrate materials. Amongst different grades of stainless steel, SS316 is most widely used because of its corrosion-resisting and high heat-resisting capacity. Nonetheless, it lacks certain mechanical and tribological properties [11]. These shortcomings can be improved by applying suitable coating on the surface. In the present study, SS316 was used as a substrate material and B_4C as coating materials were applied on the surface to improve its mechanical and tribological performance. Particle shape and chemical composition shown in Figure 4 (a, b) SS316 & (c, d) B_4C.

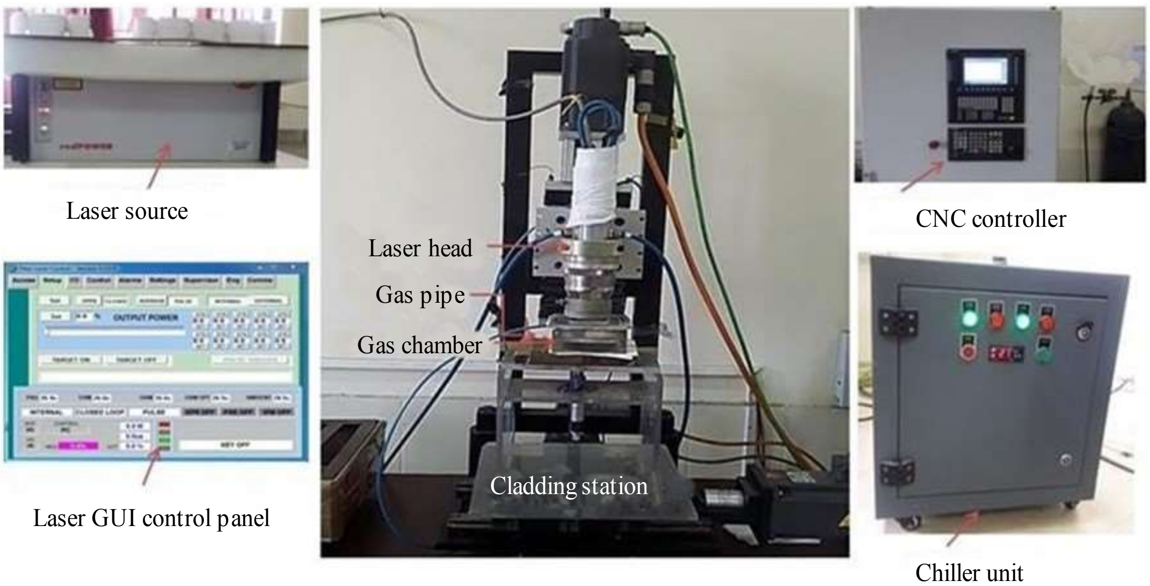

Figure 1. Shows the fiber laser cladding workstation.

ISSN: 2321-2810 (Online), ISSN: 2321-8525 (Print)

Figure 2. Graphical user interface to program the laser source unit.

Table 1. Specification of the fibre laser source.

Make	**SPI UK**
Power	50-400W
Wavelength	1070 ± 10 nm
Mode of operation	Continuous-wave
Beam profile	Gaussian
Full angle divergence	< 0.45 mrd

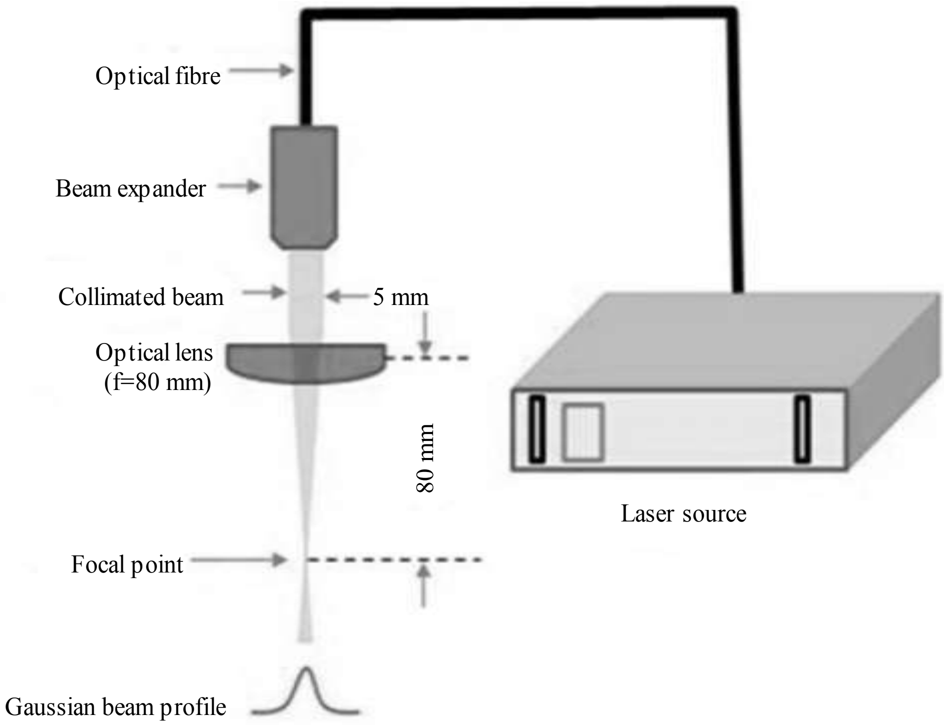

Figure 3. Depicts the laser source and beam delivery system.

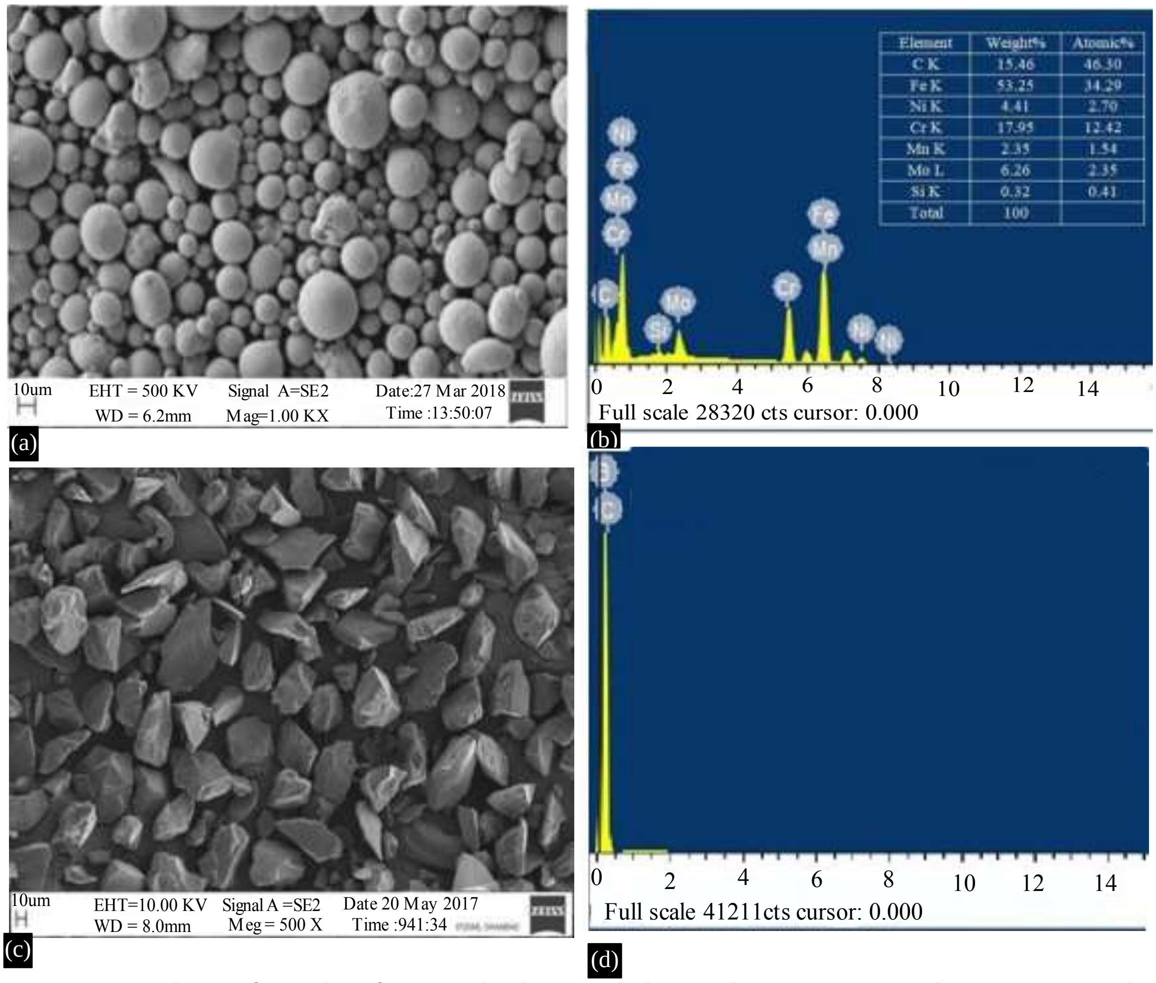

Figure 4. Analysis of powders for particle shape and chemical composition (a, b) SS316 & (c, d) B_4C

Input process Parameters

Scanning speed (mm/min), laser power density (w), volume % of different powder mixtures, laser spot diameter, hatching gap, layer thickness and beam path overlap were the available process parameters for all the studies. The range of potential process parameters needed to obtain a satisfactory surface clad was determined by conducting several trials experiments. However, with the variation of powder and their composition, the input parameters have been varied as per the requirement, to get the effective cladding.

Design of Experiments and Parameter Settings

By considering the value of process parameters (working range) from trial runs, the experimental table was design, using MINITAB-17 statistical software according to the response surface methodology. The variable process parameters, considered for the experiment design, were the laser beam scanning speed (mm/min), laser power (w), and % v/v of different powder mixtures. On the other hand, the constant parameters comprised the laser spot diameter, hatching gap, layer thickness, and beam path overlap. Table 2 shows the parameters and their respective level. A central composite design (CCD) was chosen where 2n number base points were augmented by an additional 2n central point and 2n number of axial points, being the number of variables. In this study, three variable process parameters were considered, i.e., laser power (W), scanning speed (mm/min), and % v/v composition of B_4C particulates, resulting in 8 base points along with 6 axial points and 6 central points. A total of 20 experimental runs were conducted with 1 block and 1 replication. Table 3 shows the complete parameter settings for different experimental runs and corresponding measured response data.

Experimental Methods

A CNC program was developed to demarcate the prepared powder-layered surface area, which had to be scanned by laser beam. A laser beam was panned over the preplaced surface in a way that two consecutive laser beam-scanning paths overlapped by 50%, shown in Figure 5. The obtained clad surface was further characterized by different techniques, which has been discussed in the next Section.

Characterization Techniques

For characterization, the laser clad surface was sectioned (out a 4x4 mm^2 area from the parent) using wire electrical discharge machining (WEDM). Thereafter, it cleans thoroughly with acetone, followed by ultrasonic vibration to insure free from any unbound powder particles on the clad surface. Now to obtain uniform surface finish of the cut sample, a mould was prepared by inserting the clad cut-section in the center (Using mould making machine, Make: Chennai Metco, India). After that, prepared mouldwere polished using emery paper of various mesh size. Afterwards, diamond paste was applied to the sample in order to give it an overall mirror finish, followed by an acetone bath. In order to prepare them for etching, the samples were dried with an industrial dryer following this. In the next step, the samples were etched with Kroll's reagent (HF:HNO3:H2O :: 1:3:9) for around 10-20 seconds. In order to measure the microhardness of the clad surface, a Vickers microhardness tester was used (model: Economet VH-1 MD, manufacture: Chennai Metco, India. The micro-hardness value was not uniform throughout the surface which could be due to the formation of different intermetallic insetu carbides, such as, FeC, CrC and B_4C.

RESULTS AND DISCUSSION

Microstructure Analysis of the Clad Surfaces

Figure 6 shows the optical image of clad surface, it indicates the dispersion of B_4C particles in the matrix of SS316 without any dilution. The FESEM examination also revealed the absence of micro or macro cracks on the surface of the clad layer and shown in Figure 7. Obtained clad surface are also free from any fine gaps between boron carbide and SS316 indicates their good wettability. Figure. 8 (a), (c) shows the cross-section of B_4C & SS316 surface and (b), (d) shows the EDX analysis on the SS316 surface parts and B_4C sides.

Table 2. Parameters and their respective level.

Parameters	Units	Levels		
		+1.681+10-1-1.681		
Scanning Speed	mm/minute	100	175	250
Laser Power	Watt	50	150	250
Composition	Volume (% v/v)	5	15	25
Powder layer thickness: 0.4 mm, hatching line gap: 0.2 mm, laser beam spot diameter: 0.4 mm and beam path overlapping: 50%				

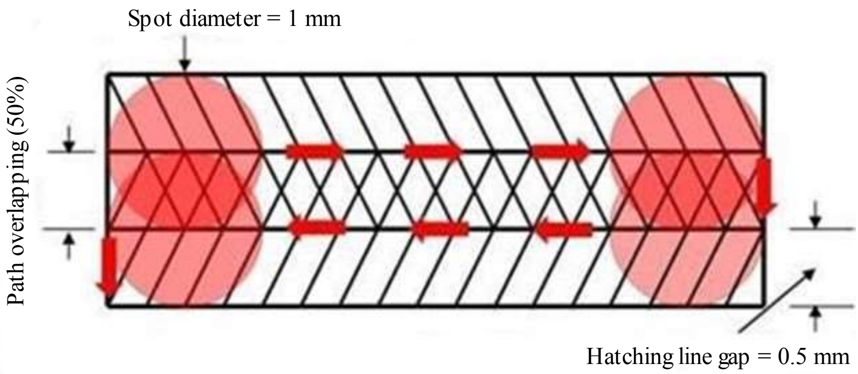

Figure 5. Path of the laser beam with a 50% overlap [12].

Table 3. Developed design matrix with the respective responses.

S no.	Process parameters			Responses					
	Scanning speed (mm/min)	Power (W)	Composition (%v/v)	Average hardness ($HV_{0.2}$)		Coefficient of friction		Clad layer thickness(mm)	
				Actual	Predicted	Actual	Predicted	Actual	Predicted
1	175	234	15	294	285.394	0.387	0.381	0.337	0.325
2	217.04	150	15	284	280.152	0.335	0.337	0.331	0.372
3	150	200	20	264	262.559	0.412	0.416	0.326	0.312
4	175	66	15	252	260.089	0.303	0.315	0.314	0.354
5	150	100	20	283	286.780	0.445	0.443	0.329	0.300
6	200	200	10	281	278.519	0.387	0.383	0.394	0.364
7	175	150	15	262	261.543	0.432	0.432	0.297	0.338
8	150	100	10	262	262.802	0.286	0.320	0.343	0.370
9	175	150	6.5	253	248.935	0.303	0.295	0.358	0.346
10	175	150	23.4	258	255.053	0.402	0.411	0.232	0.287
11	200	200	20	274	278.681	0.361	0.367	0.373	0.360
12	132.95	150	15	264	262.802	0.317	0.320	0.384	0.368
13	175	150	15	263	262.802	0.323	0.320	0.362	0.369
14	175	150	15	256	252.023	0.418	0.411	0.372	0.360
15	175	150	15	274	262.802	0.289	0.320	0.379	0.367
16	175	150	15	281	287.582	0.334	0.340	0.393	0.380
17	150	200	10	263	262.802	0.342	0.320	0.387	0.366
18	200	100	10	258	260.232	0.371	0.355	0.372	0.344
19	175	150	15	252	251.059	0.332	0.329	0.327	0.300
20	200	100	20	287	289.802	0.362	0.320	0.356	0.370

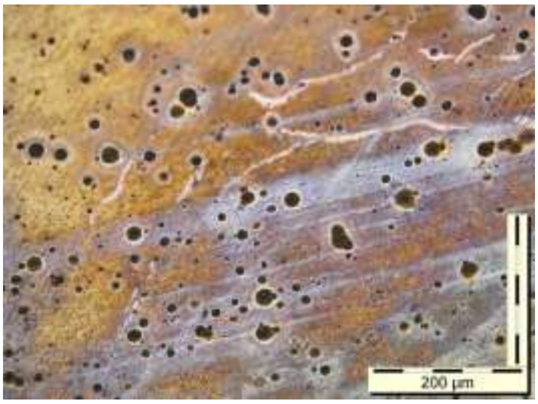

Figure 6. Optical image of clad sample show the disperse B_4C particulate on the substrate surface.

Model Fitting and Statistical Analysis

After conducting all the experiments, the responses were measured and entered with the help of Minitab-17 software, and model fitting was carried out. A second-order regression equation was formulated to correlate the input variables with the responses. Equations 2, 3, and 4 represent the regression model in uncoded form for the average micro-hardness, coefficient of friction, and clad layer thickness. Analysis of variance (ANOVA) was done for each of the responses, the result of which is presented in Tables 4, 5, and 6. To find the significant input process parameters as well as their square terms and interactions, F-test and P-test were conducted with the software and summarized in Table 7. Higher F-value and P-value ≤ 0.05 indicated the significant contribution of the individual term of regression equation in achieving the responses. The insignificant terms were removed from the equation [13-18].

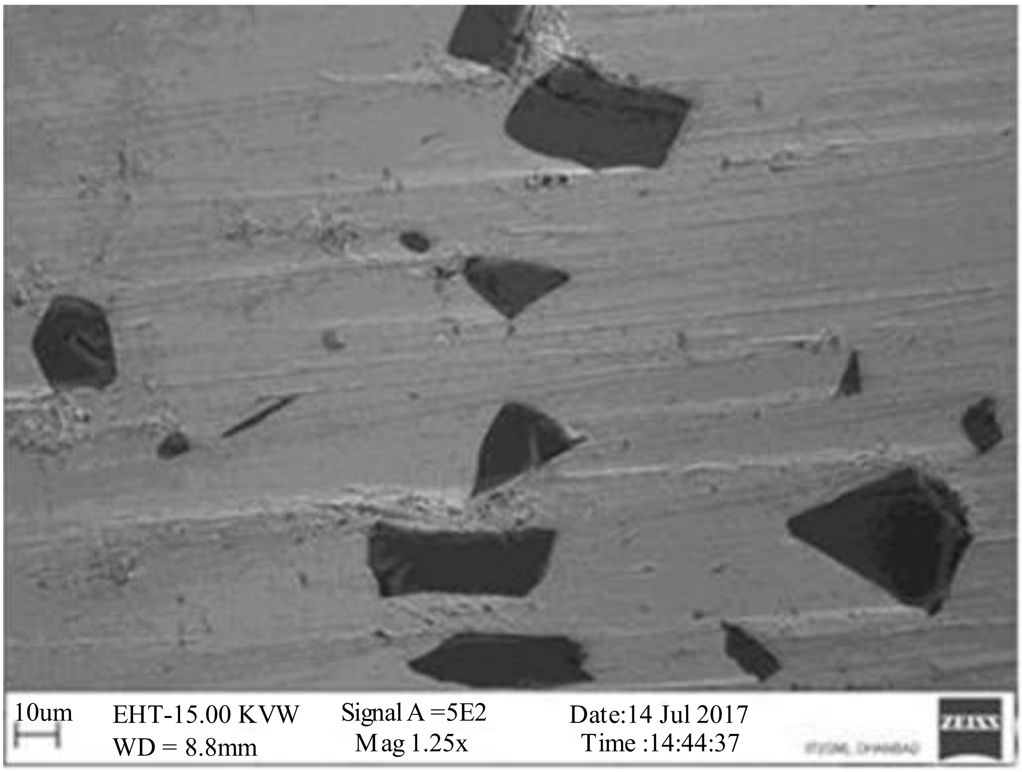

Figure 7. FESEM micrograph of clad surface showing the uniform distribution of B_4C particles on the clad surface

$$Y_1 = 367 + 0.84 X_1 -1.433X_2-1611 X_3 + 0.00118 X_1^2 +0.004820 X_2^2 +0.5810 X_3^2-0.0040 X_1*X_2-0.0320 X_2*X_3+0.053 X_1*X_3 \quad \text{(Eq 2)}$$

$$Y_2= 1.615-0.00881X_1-0.00279X_2-0.0359X_3+ 0.000027 X_1^2+0.000010 X_2^2 +0.000793 X_3^2 -0.000029 X_2*X_3 \quad \text{(Eq 3)}$$

$$Y3=0.587 - 0.004258 X_1 + 0.001042 X_2 + 0.01161 X_3+ 0.000013 X_1^2 - 0.000001 X_2^2 -0.000610 X_3^3 - 0.000003 X_1*X_2-0.00001X_2*X_3 \quad \text{(Eq 4)}$$

where, X_1, X_2 and X_3 represent the laser beam scanning speed (mm/min), laser power (W) and composition (%v/v), respectively; Y_1, Y_2 and Y_3 represent the average micro-hardness ($HV_{0.2}$), coefficient of friction and clad layer thickness (mm), respectively.

ANOVA for average micro-hardness was carried out at 95% of confidence level as shown in Table 4. The F- value of the model was 31.76, indicating that the model was significant. The significant terms in the regression equation were X_1, X_2, X_3, quadratic terms such as $X1^2$, $X_2{}^2$, $X3^2$, and interaction terms such as X_1*X_2, X_2*X_3, and X_1*X_3. For all these terms, the P-value was<0.05, which indicates that these are significant parameters. The values of R2, adjusted R2, and predicted R2 were 96.62%, 93.58%, and 90.29%, respectively, which implies that the model has good prediction ability within the preview of the selected parameter ranges. Table 5 shows ANOVA for the coefficient of friction at 95% of the confidence level. The model had an F value of 31.76, which implies that it is significant.

The regression equation was developed and the significance of each term was checked. The terms having a p-value < 0.05 were kept in the equation and other terms were considered as insignificant, hence, removed.

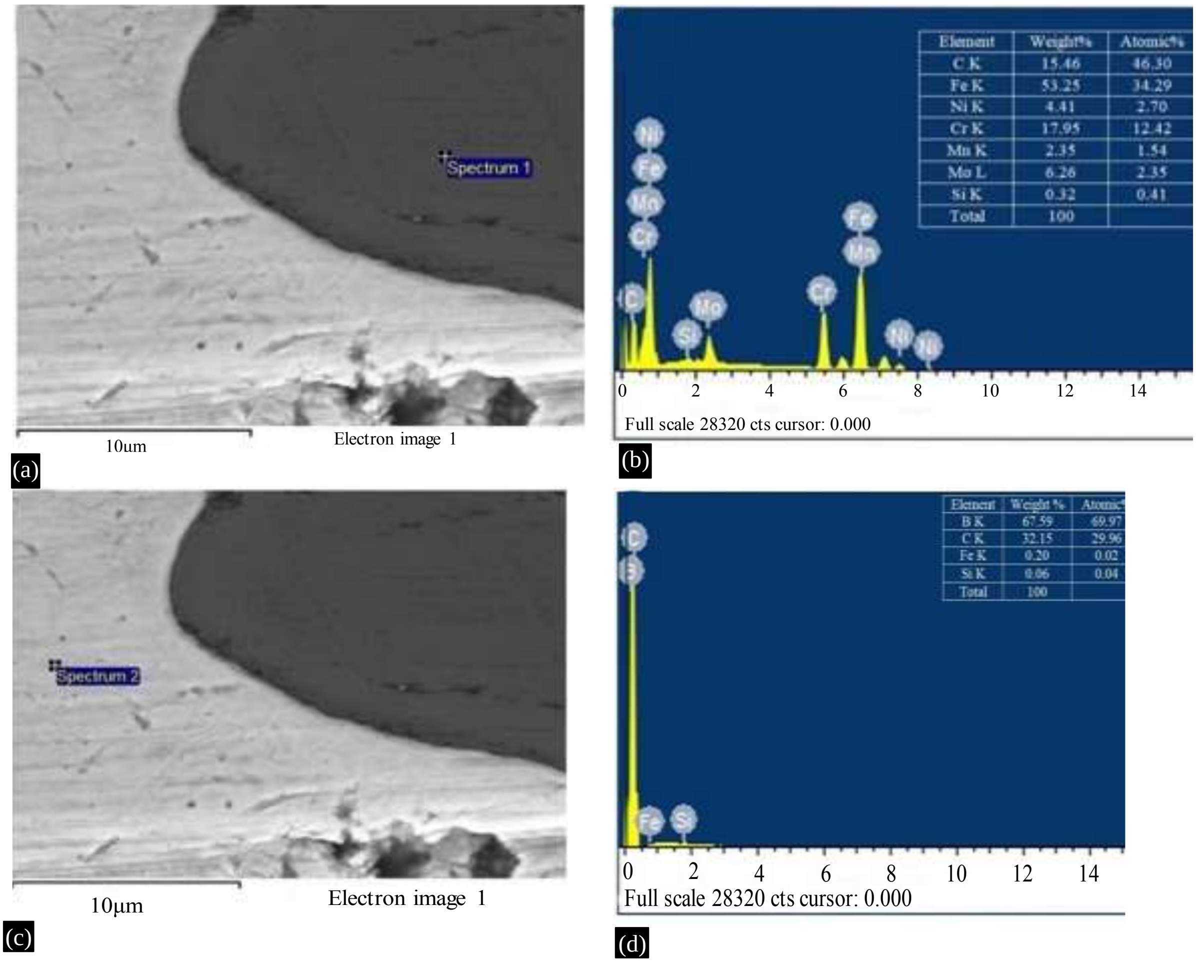

Figure 8. (a) & (c) FESEM micrograph of clad cross-section and (b) & (d) EDX analysis on SS316 surface & B_4C surface.

Table 4. ANOVA test for average micro-hardness.

X_1: Scanning Speed (mm/min) X_2: Laser Power (W) X_3: Composition of B_4C (%v/v)					
Source	***DF***	***Adj SS***	***Adj MS***	***F-Value***	***P-Value***
Model	9	3001.00	333.44	31.76	0.000
Linear	3	1733.58	577.86	55.04	0.000
X_1	1	1247.00	1247.00	118.77	0.022
X_2	1	101.23	101.23	9.64	0.048
X_3	1	385.36	385.36	36.70	0.000
Square	3	860.05	286.68	27.30	0.000
X_1^2	1	180.18	180.18	17.16	0.121
X_2^2	1	281.52	281.52	26.81	0.031
X_3^3	1	551.76	551.76	52.55	0.010
2-Way Interaction	3	407.38	135. 79	12.93	0.001
X_1X_2	1	28.13	28.13	2.68	0.033
X_2X_3	1	1.12	1.12	0.11	0.000
X_1X_3	1	378.13	378.13	36.01	0.000
Error	10	105.00	10.50		
Lack-of-Fit	5	23.66	4.73	0.29	0.899
Pure Error	5	81.33	16.27		
Total	19	3106.00			
S: 3.240, R-sq: 96.62%, R-sq(adj): 93.58% and R-sq(pred): 90.29%					

ISSN: 2321-2810 (Online), ISSN: 2321-8525 (Print)

Table 5. ANOVA test for coefficient of friction.

Source	DF	Adj SS	Adj MS	F-value	P-value
Model	9	0.027	0.003	45.60	0.000
Linear	3	0.013	0.004	66.40	0.000
X_1	1	0.000	0.000	10.88	0.008
X_2	1	0.002	0.002	31.87	0.000
X_3	1	0.010	0.010	156.43	0.000
Square	3	0.004	0.001	21.81	0.000
X_1^2	1	0.000	0.000	2.29	0.161
X_2^2	1	0.003	0.003	46.42	0.00
X_3^2	1	0.001	0.001	24.91	0.001
2-Way Interaction	3	0.009	0.003	48.60	0.000
X_1X_2	1	0.000	0.000	0.76	0.403
X_2X_3	1	0.001	0.001	18.29	0.002
X_1X_3	1	0.008	0.008	126.75	0.000
Error	10	0.000	0.000		
Lack-of-Fit	5	0.000	0.000	5.08	0.049
Pure Error	5	0.000	0.000		
Total	19	0.027			
S : 0.008, R-sq : 97.62%, R-sq(adj) : 95.48%, R-sq(pred) : 84.00%					

Table 6. ANOVA test for clad layer thickness.

Source	DF	Adj SS	Adj MS	F-Value	P-Value
Model	9	0.014	0.001	46.96	0.000
Linear	3	0.009	0.002	90.79	0.000
X_1	1	0.000	0.000	0.80	0.000
X_2	1	0.000	0.000	17.72	0.029
X_3	1	0.008	0.008	253.85	0.001
Square	3	0.004	0.001	47.71	0.000
X_1^2	1	0.000	0.000	28.61	0.034
X_2^2	1	0.000	0.000	0.95	0.011
X_3^2	1	0.003	0.003	102.07	0.048
2-Way Interaction	3	0.000	0.000	2.40	0.129
X_1X_2	1	0.000	0.000	4.14	0.000
X_2X_3	1	0.000	0.000	1.68	0.000
X_1X_3	1	0.000	0.000	1.37	0.107
Error	10	0.000	0.000		
Lack-of-Fit	5	0.000	0.000	1.68	0.292
Pure Error	5	0.0001	0.000		
Total	19	0.014			
S:0.006, R-sq : 97.69% , R-sq(adj): 95.61% , R-sq(pred): 87.77%					

The value of R^2, adjusted R^2, and predicted R^2 were 97.62%, 95.48%, and 84.00%, respectively, which proves the prediction ability of the regression equation. This is because sufficient heat input around the clad zone enables the development of new bonds between the clad materials and the substrate surface and leads to the formation of new and hard compounds. On the other hand, at higher % composition, the micro-hardness shows a declining trend after a few points of % composition. This could be explained by the fact that insufficient heat input at the clad surface hinders the initiation and progress of chemical reactions between the powder particles. This is because sufficient heat input around the clad zone enables the development of new bonds between the clad materials and the substrate surface and leads to the formation of new and hard compounds. On the other hand, at higher % composition, the micro-hardness shows a declining trend after a few points of % composition. This could be explained by the fact that insufficient heat input at the clad surface hinders the initiation and progress of chemical reactions between the powder particles. Figure 9 (c) indicates that the maximum micro- hardness of 281HV0.2 can be achieved at a scanning speed of 175 mm/min, laser power of 150W, % composition of 15% v/v. The micro-hardness gets reduced if there is any variation in values of the said parameters. In view of the above analysis, laser power and % composition of B_4C can be said to play a major role in achieving a greater hardness as compared to other combinations of the experimental process parameters. Figure 9 (d, e, and f) shows the variation in coefficient of friction with respect to the combination of any two of the input process parameters. In the purview of the present research, the coefficient of friction is in the range of 0.29-0.5. In fig. 9 (d), one can notice that the minimum coefficient of friction can be achieved when the laser power and scanning speed are in the range of 90-207 W and 135-207 mm/min at a constant volume % of B_4C (15% v/v). The same value of 0.29 can be achieved when the % composition and laser power are in the range of 18 - 23% v/v and 150-170 W, respectively, at 175 mm/min of scanning speed [Figure 9 (f)]. The above observations could perhaps be explained by the fact that the density of B_4C is lower than the density of the material present in the clad zone. As a result, B_4C particles remain on the clad. This could be explained by the fact that insufficient heat input at the clad surface hinders the initiation and progress of chemical reactions between the powder particles. Figure 9 (c) indicates that the maximum micro- hardness of $281HV_{0.2}$ can be achieved at a scanning speed of 175 mm/min, laser power of 150W, % composition of 15% v/v.

The micro-hardness gets reduced if there is any variation in values of the said parameters. In view of the above analysis, laser power and % composition of B_4C can be said to play a major role in achieving a greater hardness as compared to other combinations of the experimental process parameters. Figure 9 (d, e, and f) shows the variation in coefficient of friction with respect to the combination of any two of the input process parameters. In the purview of the present research, the coefficient of friction is in the range of 0.29 - 0.5. In Figure. 9 (d), one can notice that the minimum coefficient of friction can be achieved when the laser power and scanning speed are in the range of 90-207 W and 135 - 207 mm/min at a constant volume % of B_4C (15% v/v). The same value of 0.29 can be achieved when the % composition and laser power are in the range of 18 - 23% v/v and 150-170 W, respectively, at 175 mm/min of scanning speed [Figure 9 (f)]. The above observations could perhaps be explained by the fact that the density of B_4C is lower than the density of the material present in the clad zone. As a result, B_4C particles remain on the clad surface. Similarly, the coefficient of friction value of 0.29 can be achieved when the scanning speed and % composition of B_4C are in the range of 155-190 mm/min and 18-23%v/v, respectively, at 150W laser power [Figure 9 (e)]. Moreover, if the heat input is sufficient, different intermetallic chemical compounds are formed (described in XRD Analysis Section), which leads to a low coefficient of friction. The variation of clad layer thickness with different input process parameters has been presented in Figure 9 (g, h, and i). The maximum clad layer thickness (0.387mm) obtained with three different combinations of process parameters, including, laser power and scanning speed, are in the range of 165 - 232W and 160 - 216 mm/min, [Figure 9 (g)] while % composition of B_4C and scanning speed are in the range of 11 - 23% v/v and 132 - 212 mm/min, [Figure 9 (h)]. Again, the % composition of B_4C and laser power are in the range of 13- 20% v/v and 155-232 W [Figure 9 (i)] respectively. It can also be observed from the interaction plots that the laser power and scanning speed have a significant influence on the clad layer thickness as compared to other combinations of parameters. With high scanning speed and low laser power, the layer thickness is the minimum, whereas, with high laser power, the layer thickness is the maximum. This may be due to the variation of heat input at the clad layer. More heat input leads to greater melting, thereby reducing the layer thickness. Now to observe the effects of different level of process parameter on the response are represented in Figure 10. And Figure 11 shows the normal probability distribution for hardness, coefficient of friction, clad layer thickness of the response. Form graphs, the response for individual are well fitted except few points. That may be due to error associated with materials or instruments.

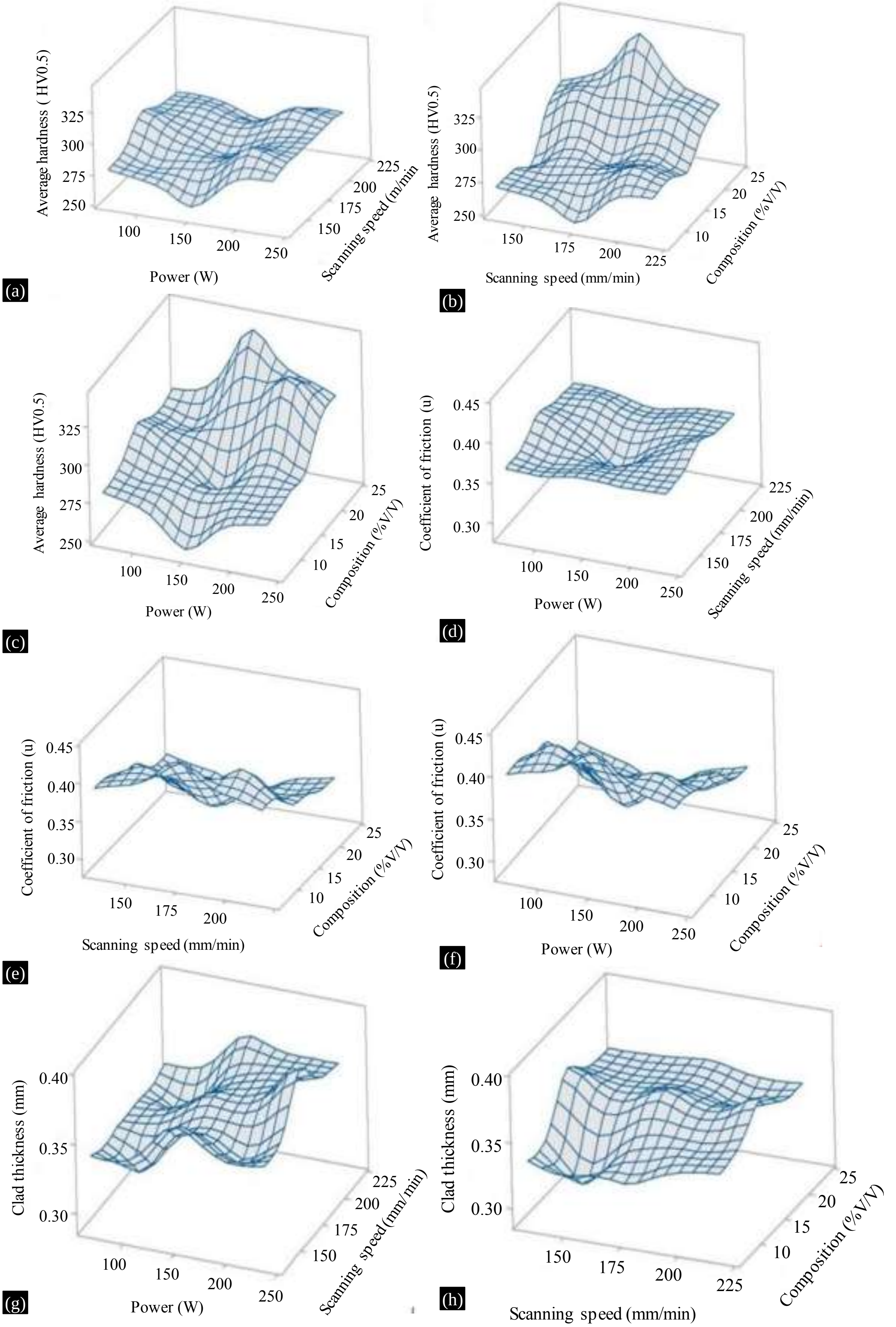
(a)
Average hardness (HV0.5)
Power (W)
Scanning speed (m/min
(b)
Average hardness (HV0.5)
Scanning speed (mm/min)
Composition (%V/V)
(c)
Average hardness (HV0.5)
Power (W)
Composition (%V/V)
(d)
Coefficient of friction (u)
Power (W)
Scanning speed (mm/min)
(e)
Coefficient of friction (u)
Scanning speed (mm/min)
Composition (%V/V)
(f)
Coefficient of friction (u)
Power (W)
Composition (%V/V)
(g)
Clad thickness (mm)
Power (W)
Scanning speed (mm/min)
(h)
Clad thickness (mm)
Scanning speed (mm/min)
Composition (%V/V)

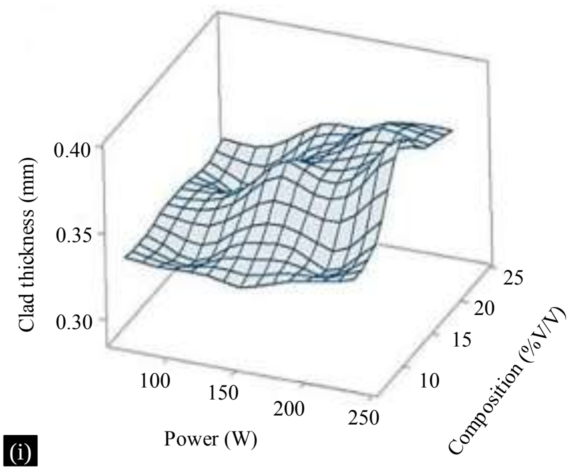

(i)

Figure 9. Response surface plots showing the effect of scanning speed, laser power and composition on (a, b and c) average micro-hardness, (d, e and f) coefficient of friction, (g, h and i) clad thickness.

Table 7. ANOVA for the quadratic polynomial model for cladded samples.

Term	P-value of the factors and their interactions		
	Average hardness	**Coefficient of friction**	**Clad layer thickness**
Scanning speed (X_1)	0.022	0.008	0.000
Power (X_2)	0.048	0.000	0.029
Composition (X_3)	0.000	0.000	0.001
X_1X_2	0.033	0.403	0.000
X_2X_3	0.000	0.002	0.000
X_3X_1	0.000	0.000	0.107
X_1	0.121	0.161	0.034
X_2^2	0.031	0.00	0.011
X_3^3	0.010	0.001	0.048
Significant if P-value < 0.05			

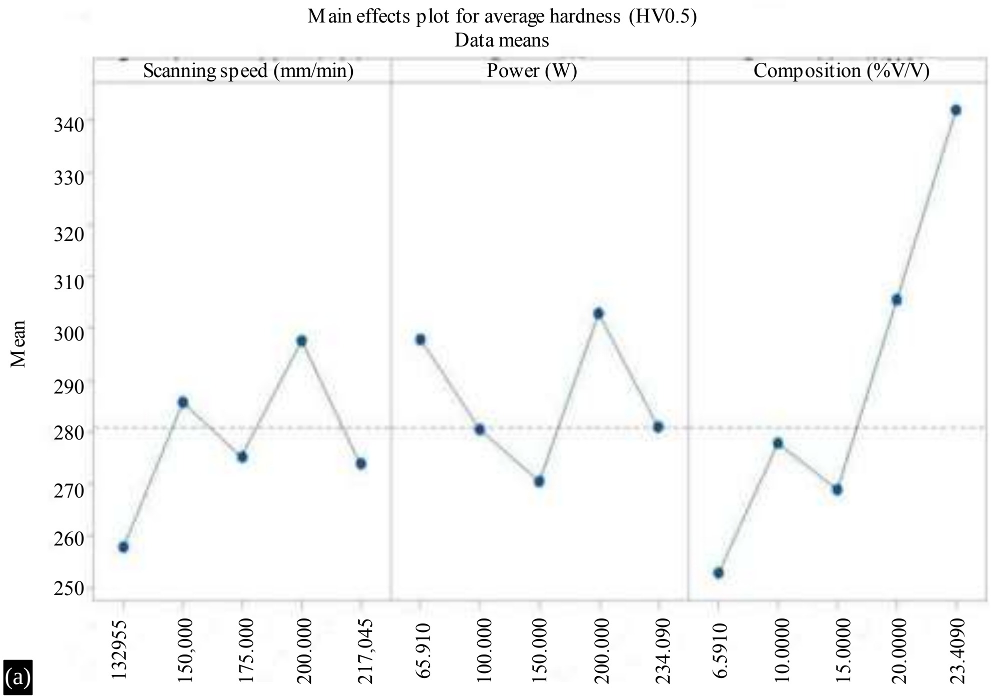

(a)

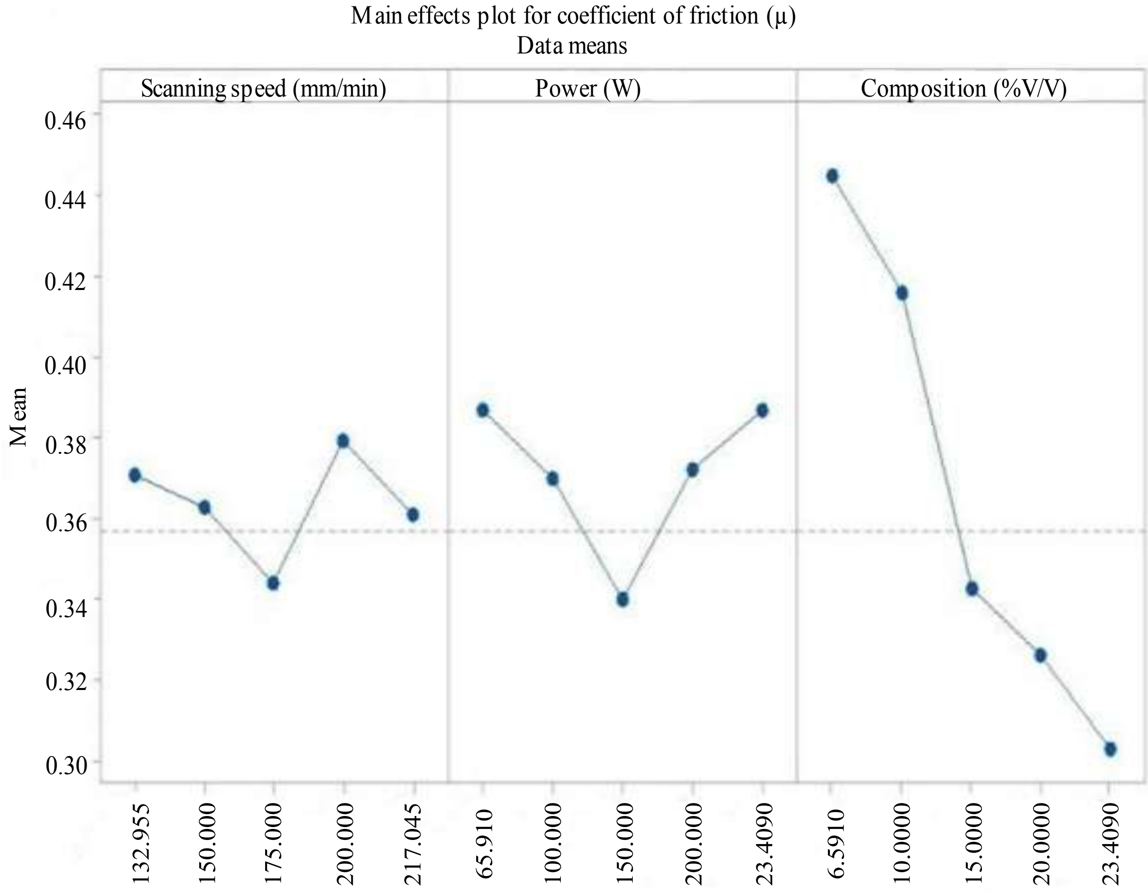

(b)

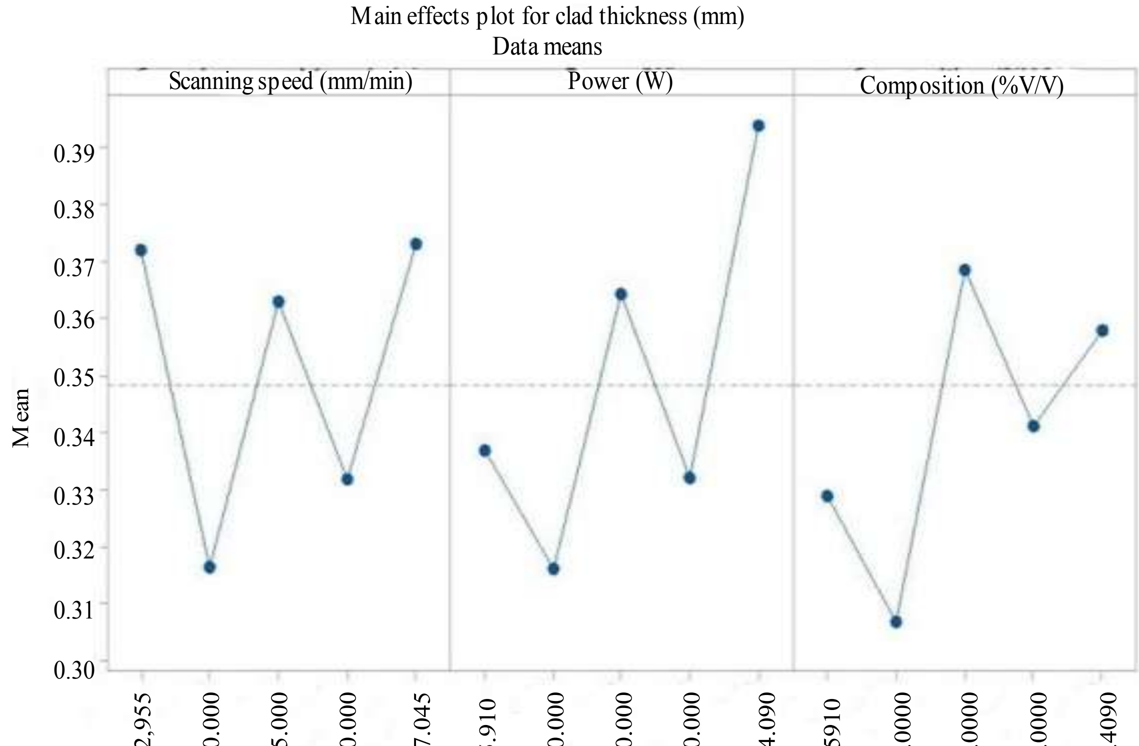

(c)

Figure 10. Main effects plot for (a) Average hardness, (b) Coefficient of friction and (c) Clad thickness.

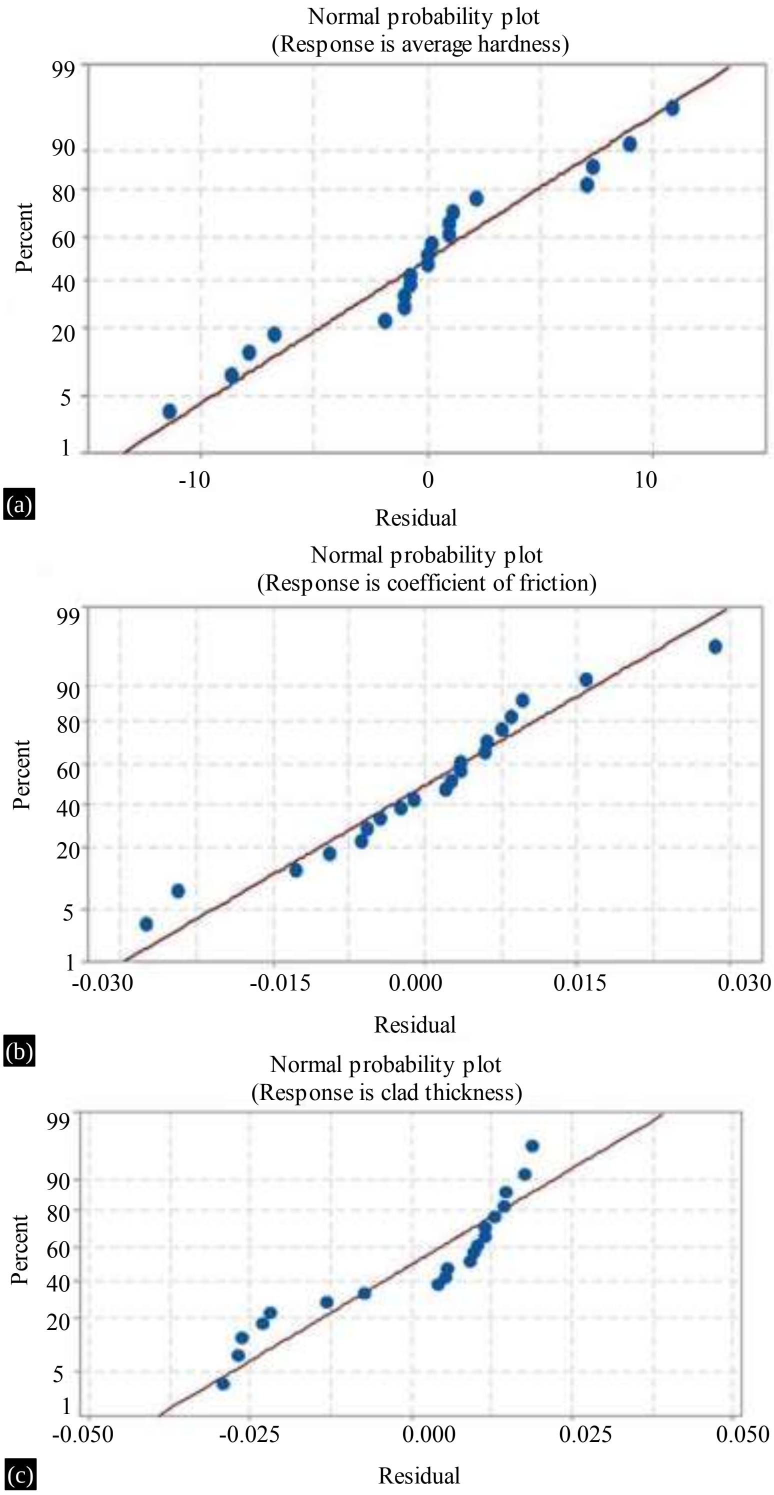

Figure 11. Normal probability plot of (a) Average hardness, (b) coefficient of friction and (c) clad thickness

CONCLUSION

Experiments on laser cladding operation were conducted successfully to prepare a clad layer, consisting of B_4C ceramic and SS316 powder, to be applied on the SS316 substrate surfaces. The RSM was applied to optimize the process and to develop a regression model for determining average micro-hardness, COF and the clad layer thickness. In addition, the surface morphology and tribological behaviour were also studied. From the analysis of results, the following conclusions are drawn: Embedment of the B_4C ceramic particles on the SS316 substrate surface has always proved to be a difficult task. Therefore, it should always be mixed with another powder so as to enable easy bonding between the substrate surface and the B_4C powder. In the present research, SS316 powder was used for this purpose and argon was used as the shielding gas. The parent SS316 surface showed an average coefficient friction of 0.510, which reduced up to 0.289, upon application of a coating of B_4C+ SS316 material, indicating the presence of the B_4C particles in the clad surface. The volume % of B_4C, laser power and scanning speed were found to be the significant parameters in the present study. Regression equations were developed and statistical validation of the model was carried out. The values of input process parameters were predicted (laser power: 200 W, scanning speed: 177.72 mm/min and composition of B_4C: 20 % v/v) for optimum responses. The response for individual are well fitted except few points through the normal probability distribution curve.

Declaration of Interest

There is no potential conflict of interest.

REFERENCES

1. Shibe V, Chawla V. A review of surface modification techniques in enhancing the erosion resistance of engineering components. International Journal of Research in Mechanical Engineering & Technology. 2014;4(2):92-5.
2. Pradeep GR, Ramesh A, Prasad BD. A review paper on hardfacing processes and materials.International Journal of Engineering Science and Technology. 2010;2(11):6507-10.
3. Ur Rahman N, Matthews DT, De Rooij M, Khorasani AM, Gibson I, Cordova L, Römer GW. An overview: Laser-based additive manufacturing for high temperature tribology. Frontiers in Mechanical Engineering. 2019 Apr 16;5:16.
4. Zhu L, Xue P, Lan Q, Meng G, Ren Y, Yang Z, Xu P, Liu Z. Recent research and development status of laser cladding: A review. Optics & Laser Technology. 2021 Jun 1;138:106915.
5. Torims T. The application of laser cladding to mechanical component repair, renovation and regeneration. Daaam international scientific book. 2013 Jan 1;12:587-608.
6. Thawari N, Gullipalli C, Chandak A, Gupta TV. Influence of laser cladding parameters on distortion, thermal history and melt pool behaviour in multi-layer deposition of stellite 6: In-situ measurement. Journal of alloys and compounds. 2021 Apr 15;860:157894.
7. M. Conduction Losses due to Part Fixturing During Laser Cladding. InThermo- Mechanical Modeling of Additive Manufacturing 2018 Jan 1 (pp. 61-79). Butterworth-Heinemann
8. Liu Y, Liu C, Liu W, Ma Y, Tang S, Liang C, Cai Q, Zhang C. Optimization of parameters in laser powder deposition AlSi10Mg alloy using Taguchi method. Optics & Laser Technology. 2019 Apr 1;111:470-80.
9. Ma M, Xiong W, Lian Y, Han D, Zhao C, Zhang J. Modeling and optimization for laser cladding via multi-objective quantum-behaved particle swarm optimization algorithm. Surface and Coatings Technology. 2020 Jan 15;381:125129.
10. Lian G, Yao M, Zhang Y, Chen C. Analysis and prediction on geometric characteristics of multi-track overlapping laser cladding. The International Journal of Advanced Manufacturing Technology. 2018 Jul;97:2397-407.
11. Liu H, Wang C, Zhang X, Jiang Y, Cai C, Tang S. Improving the corrosion resistance and mechanical property of 45 steel surface by laser cladding with Ni60CuMoW alloy powder. Surface and Coatings Technology. 2013 Aug 15;228:S296-300.
12. Misra S, Hussain M, Gupta A, Kumar V, Kumar S, Das AK. Fabrication and characteristic evaluation of direct metal laser sintered SiC particulate reinforced Ti6Al4V metal matrix composites. Journal of Laser Applications. 2019 Feb 1;31(1).
13. Krishnan MN, Suresh S, Vettivel SC, Prema CE, Arun J, Thirunamakodi P. Image Texture Description, Surface-Grains Structure Morphology and Prediction of Wear Parameters for Mg/B 4 C Composites Using Response Surface Methodology. Metals and Materials International. 2022 May 1:1-20.

14. Anderson MJ, Whitcomb PJ. RSM simplified: optimizing processes using response surface methods for design of experiments. Productivity press; 2016 Aug 5.
15. Li K, Yan S, Zhong Y, Pan W, Zhao G. Multi-objective optimization of the fiber-reinforced composite injection molding process using Taguchi method, RSM, and NSGA-II. Simulation Modelling Practice and Theory. 2019 Feb 1;91:69-82.
16. Poorvahab T, Kazemi A, Haghshenas D. Fabrication of fused silica-based cores by the gel- casting method: Modeling by response surface methodology. International Journal of Applied Ceramic Technology. 2020 Jul;17(4):1723-30.
17. Ahmad AL, Koohestani B, Bhatia S, Ooi SB. Oxidation of Styrene to Benzaldehyde by Anhydrous Hydrogen Peroxide on γ-Alumina-Supported V2O5 Nanoparticle Catalysts: Optimization Studies Using Response Surface Methodology. International Journal of Applied Ceramic Technology. 2012 May;9(3):588-98.
18. Vijayan D, Abhishek P, Kumar YM, Balaji P, kumar Reddy PS. Optimization of drilling parameters of carbon fiber composites using RSM based desirability function. InIOP conference series: materials science and engineering 2018 Jul 1 (Vol. 390, No. 1, p. 012076). IOP Publishing

